Treatment with a SOD mimetic reduces visceral adiposity, adipocyte death and adipose tissue inflammation in high fat fed mice

Karla M. Pires, **Olesya Ilkun**, **Marina Valente**, and **Sihem Boudina**

Division of Endocrinology, Metabolism and Diabetes and Program in Molecular Medicine, University of Utah School of Medicine, Salt Lake City, Utah 84112

Abstract

Objective—Obesity is associated with enhanced reactive oxygen species (ROS) accumulation in adipose tissue. However, a causal role for ROS in adipose tissue expansion after high fat feeding is not established. The aim of this study is to investigate the effect of the cell permeable superoxide dismutase mimetic and peroxynitrite scavenger Mn(III)tetrakis(4-benzoic acid)porphyrin chloride (MnTBAP) on adipose tissue expansion and remodeling in response to high fat diet (HFD) in mice.

Design and Methods—Male C57BL/6j mice were fed normal chow or high fat diet (HFD) and treated with saline or MnTBAP for 5 weeks. The effects of MnTBAP on body weights, whole body energy expenditure, adipose tissue morphology and gene expression were determined.

Results—MnTBAP attenuated weight gain and adiposity through a reduction in adipocyte hypertrophy, adipogenesis and fatty acid uptake in epididymal (eWAT) but not in inguinal (iWAT) white adipose tissue. Furthermore, MnTBAP reduced adipocyte death and inflammation in eWAT and diminished circulating levels of free fatty acids and leptin. Despite these improvements, the development of systemic insulin resistance and diabetes after HFD was not prevented with MnTBAP treatment.

Conclusions—Taken together, these data suggest a causal role for ROS in the development of diet-induced visceral adiposity but not in the development of insulin resistance and type 2 diabetes.

Keywords

Adipose tissue; adipogenesis; oxidative stress; superoxide dismutase; mitochondrial dysfunction; insulin resistance

---

Corresponding author: Sihem Boudina, Address: Division of Endocrinology, Metabolism and Diabetes, Program in Human Molecular Biology & Genetics, 15 N 2030 E Bldg # 533 Rm. 3410B, Salt Lake City, Utah 84112, Phone: (801) 585-6833, Fax: (801) 585-0701, sihem.boudina@hmbg.utah.edu.

Conflict of interest statement: The authors declared no conflict of interest.

Introduction

Obesity rates are increasing in the United States, estimating more than 35.7% of adults and 16.9% of children and adolescents are considered obese (1). Obesity is a risk factor for insulin resistance, the metabolic syndrome and cardiovascular disease (2). Unfortunately, obesity rates keep increasing because more and more children are becoming overweight or obese due to a sedentary lifestyle characterized by excess consumption of highly processed and energy-dense food. Furthermore, current strategies aimed to limit obesity such as weight loss programs have proven ineffective due to rapid weight re-gain. Thus, developing new treatments for obesity is urgent.

Obesity is associated with increased systemic and adipose tissue oxidative stress (3). Indeed, Furukawa et al. (4) showed that adipose tissue of genetically obese or diet-induced obese animals produced higher amounts of hydrogen peroxide (H_2O_2), have reduced antioxidant enzyme activity and enhanced mRNA level of nicotinamide adenine dinucleotide phosphate (NADPH) oxidase subunits. Furthermore, lower levels of glutathione peroxidase 3 (GPx3) and reduced activity were observed in white adipose tissue (WAT) of genetically obese *ob/ob* and *db/db* mice (5). These data suggest that reactive oxygen species (ROS) are locally produced in adipose tissue and may play a role in the pathogenesis of obesity.

There has been substantial interest in using natural antioxidants for the treatment of obesity and the associated insulin resistance and the metabolic syndrome. Metalloporphyrins have been shown to mimic the biochemical activity of superoxide dismutase (SOD) (6) and were found to substitute for it in mutant prokaryotes lacking SOD (7). Day et al. (8) showed that MnTBAP was effective in attenuating paraquat-induced endothelial cell injury *in-vitro* and protecting paraquate-induced lung injury *in-vivo* (9).

We previously showed that protection from diet-induced oxidative stress through increased skeletal muscle mitochondrial uncoupling is sufficient to reduce weight gain but failed to prevent the development of insulin resistance in FVB mice (10). Therefore, this study was designed to investigate whether pharmalogical reduction of oxidative stress limits adiposity, ameliorates the metabolic disturbances and reverses insulin resistance and diabetes associated with high fat feeding in mice. Here, we demonstrated that protection from oxidative stress limited visceral adiposity and adipose tissue remodeling but failed to prevent diet-induced insulin resistance and diabetes in mice.

Methods and Procedures

Animals, diet and treatment

The investigation conforms to the Guide for the Care and Use of Laboratory Animals published by the US National Institutes of Health (NIH Publication No. 85–23, revised 1996) and was approved by the Institutional Animal Care and Use Committee of the University of Utah. Male C57BL/6J mice (The Jackson Laboratory, Bar Harbor, Maine) were fed high fat diet (HFD) or normal chow (NC) for 5 weeks. At the start of the diet, mice received an intra-peritoneal injection of saline (0.9% w/v NaCl) or MnTBAP (20 mg/kg body weight) three times a week for 5 weeks. As detailed in Supplementary Table 1, the %

Kcal for the NC diet is 34% carbohydrates, 53% proteins and 13% fat (soybean oil) whereas and for the HFD is 20% carbohydrates, 35% proteins and 45% fat (soybean oil and lard).

Oxidative stress detection

Superoxide production was monitored by the superoxide detector MitoSOX Red (Life Technologies, Grand Island, NY). Freshly isolated epididymal white adipose tissue (eWAT) was sectioned and incubated with MitoSOX Red (50 μmol/L) for 30 minutes at 37°C. Fluorescence (expressed as % red) was quantified in three low-power field images from five animals in each group. Reduced and oxidized glutathione content in eWAT homogenates was determined using a spectrophotometric assay kit (EMD Millipore, Billerica, MA).

Body composition

Mice were anesthetized by a single intra-peritoneal injection of 400 mg chloral hydrate/kg body weight. Fat mass and lean mass were determined using Dual Energy X-Ray Absorptiometry (DEXA) (Norland Medical Systems, Fort Atkinson, WI).

Indirect calorimetry

Mice housed for 72 hours in a four-chamber Oxymax system (CLAMS; Columbus Instruments, Columbus, OH) as previously described (11). O_2 and CO_2 content of the exhaust air from each chamber was compared with ambient air O_2 and CO_2 content. Food consumption was monitored by electronic scales, water by electronic sipper tubes, and movement by XY/Z laser beam interruption. Respiratory exchange ratio (RER) was calculated as VCO_2/VO_2.

Adipocyte diameter

Adipocyte diameter was measured using live tissue imaging as described by Nishimura et al. (12). Briefly, eWAT was removed (∼3 mm each), washed and incubated with 5 μmol/mL boron-dipyrromethene BODIPY (Life Technologies, Grand Island, NY). Nuclei were counterstained with 40 μmol/L 4′-6-Diamidino-2-phenylindole (Hoechst 33258, Sigma-Aldrich, St. Louis, MO). Images were acquired with a confocal laser-scanning microscope (FV1000-XY- Olympus IX81). Each resulting image was created from the average of ten frames and processed to produce a surface-rendered three-dimension picture. Ten low-power field images were acquired at regular intervals from five animals in each group. The major and minor adipocyte diameters (μm) were measured to determine the mean diameter using the Image Pro-Plus software (Image-Pro Plus version 7.0., Media Cybernetics, Silver Spring, MD).

Adipocyte death

Sections of eWAT were co-incubated with the green-fluorescent probe YO-PRO-1 (0.2 μmol/L, Life Technologies, Grand Island, NY) and the red dye propidium iodide (PI), (0.3 μg, Life Technologies, Grand Island, NY). Nuclei were co-stained with 40 μmol/L Hoechst (Sigma-Aldrich, St. Louis, MO). Apoptotic cells show green fluorescence, and dead cells show primarily red fluorescence. At least 1000 nuclei were counted per animal for three animals per group at randomly chosen sections.

Crown-like structures quantification

Tissue samples from eWAT were fixed in formaldehyde (4% w/v in 0.1 mol/L phosphate buffer pH 7.2) for 48 hours, dehydrated, embedded in paraplast plus (Sigma-Aldrich, St. Louis, MO), sectioned at 5 μm and stained with hematoxylin and eosin (Sigma-Aldrich, St. Louis, MO). Five non-consecutive microscopic fields were analyzed per animal for a total of four animals per group on a light microscope (Olympus IX71 Olympus Inc., Japan).

Serum metabolites, hormone levels and glucose and insulin tolerance tests

Glucose tolerance test (GTT) and insulin tolerance tests (ITT) were performed after 6 hours fat for GTT and in random-fed animals for ITT as previously described (10). Fasting (6 hours) blood glucose, insulin, free fatty acid (FFA), triglycerides (TG), leptin and adiponectin levels were determined as previously described (10).

Mitochondrial respiration

Mitochondrial function was studied using the saponin-permeabilized fiber technique with succinate (5 mM) and rotenone (10 μM) as previously described (13).

Reverse transcription-polymerase chain reaction (RT-PCR)

Total RNA was extracted from epididymal and inguinal white adipose tissue with TRIzol reagent and purified with the RNeasy kit (QIAGEN, Valencia, CA). Equal amounts of RNA were subjected to real-time PCR using an ABI Prism 7900HT instrument in 384-well plate format with SYBR Green I chemistry and 6-carboxyl-X-rhodamine internal reference. Primer sequences are provided in Supplementary Table 2.

Statistical analysis

All data are expressed as means ± SEM. The significance of differences was determined by the use of an unpaired, two-tailed Student t test when only two groups were compared or a two-way ANOVA followed by a Bonferroni post hoc analysis when significant interaction occurred since two variables were considered: diet and treatment. Frequency of incidence of either apoptotic or necrotic nuclei number and the total nuclei number were calculated by the Chi-squared test with one degree of freedom.

Results

MnTBAP treatment reduced HFD-induced oxidative stress in eWAT

Short-term HFD resulted in a significant ($p<0.05$ vs NC saline) increase in superoxide generation in eWAT (Figure 1a, b) which was associated with a reduction in the ratio of reduced (GSH)/oxidized (GSSG) glutathione (Supplementary Figure S1a, b). MnTBAP treatment prevented superoxide generation in eWAT as suggested by the reduction in MitoSOX straining ($p=0.06$ vs HF saline). To investigate whether increased oxidative stress was due to reduced antioxidant defense, mRNA levels of MnSOD (Sod2), NADPH oxidase subunit 4 (NOX4), Cu/ZnSOD (Sod1) and glutathione peroxidase 4 (GPX4) were measured. While no change was observed for NOX4, Sod1 and GPX4, Sod2 expression in eWAT was

enhanced with HFD and reduced by MnTBAP (Figure 1c, d and supplementary Figure 1b, c).

MnTBAP reduced HFD-induced adiposity

HFD (45% in fat content) resulted in a modest 11% ($p<0.05$ vs NC saline) increase in body weight that was completely prevented by MnTBAP treatment (Figure 2a). Despite a modest weight gain, body composition was significantly altered by HFD as evidenced a 2 fold ($p<0.005$ vs NC saline) increase in fat mass whereas lean mass was unchanged (Figure 2b, c). MnTBAP treatment significantly attenuated adiposity in HF-fed mice as evidenced by reduced fat mass (Figure 2c), an effect that persisted even when lean and fat mass were expressed as percentage of body weights (data not shown). It should be noted that MnTBAP-treated HF-fed animals exhibited a slight but significant increase in lean mass relative to saline-treated mice fed the same diet (Figure 2b). Next, we sought to determine whether MnTBAP reduced fat pads weight and found that HFD-induced expansion of brown adipose tissue (BAT) and eWAT was attenuated with MnTBAP treatment (Figure 2d, f). Interestingly, the effect of MnTBAP is depot-specific as inguinal and perirenal weights, which were increased by HFD were unaffected by MnTBAP (Figure 2e, g).

MnTBAP effects on adiposity are independent of food intake, substrate oxidation or physical activity

The reduction in weight gain with MnTBAP could be due to either a decrease in energy intake or an increase in energy expenditure. To address that, we measured oxygen consumption (VO_2), carbon dioxide release (VCO_2), food intake and movement. VO_2 was not statistically different between the groups (Figure 3a), whereas VCO_2 was reduced in HF-fed saline-treated group but not MnTBAP-treated group (Figure 3b). Upon HFD, oxidation of fatty acids increased as evidenced by the reduction of RER. Despite no alterations in VCO_2 with MnTBAP treatment, RER was still reduced, suggesting that substrate preference was not altered by the treatment (Figure 3c). However, there was a slight but significant ($p<0.05$) increase in RER during the day in the NC-fed animals treated with MnTBAP, suggesting increased carbohydrates utilization (Figure 3c). Furthermore, energy expenditure was unaffected by MnTBAP as heat production was indistinguishable between the groups (Figure 3d). Finally, neither food intake nor physical activity was altered by MnTBAP treatment (Supplementary Figure 2).

MnTBAP reduced adipocyte hypertrophy, adipogenesis and fatty acid uptake in eWAT

Because there was no change in energy intake or expenditure, other mechanisms were explored to explain the reduction in adiposity following MnTBAP treatment. First, we performed morphometric analysis of eWAT and found that while MnTBAP had no effect on adipocyte number (Data not shown), it significantly affected adipocyte distribution and diameter. Thus, short-term HFD resulted in a 2 fold ($p<0.005$) increase in the average adipocyte diameter compared to NC-fed saline (75 ± 3.3 μm vs 37 ± 9.4 μm) and caused a significant shift toward larger adipocytes (Figure 4a, b). Treatment with MnTBAP prevented this shift, restored the normal distribution of adipocyte size and significantly ($p<0.005$) reduced the mean diameter. It is worth noting that MnTBAP caused a slight but significant increase in the average adipocyte diameter in NC-fed animals (Figure 4a, b). Next, we

examined the effect of MnTBAP on adipogenesis and fat uptake in eWAT and found that consistent with prior reports (14, 15), HFD enhanced adipogenesis in eWAT as evidenced by the significant ($p < 0.05$) increase in mRNA expression of key adipogenic genes such as PPARγ and aP2 (Figure 4c), an induction that was prevented with MnTBAP. Interestingly, these changes in adipogenesis were not observed in iWAT (Supplementary Figure 3), suggesting a depot-specific effects of HFD and MnTBAP. Furthermore, and consistent with increased adipocyte diameters in eWAT of HF-fed saline-treated mice, there was an induction of mRNA expression of fatty acid translocase CD36, suggesting a higher fat uptake in this depot (Figure 4d), an effect that was attenuated with MnTBAP treatment.

MnTBAP treatment attenuated the effects of HFD on de novo lipogenesis

In addition to adipogenesis and fat uptake, we also assessed the expression of genes involved in fatty acid oxidation, lipolysis and de novo lipogenesis. HFD was associated with a significant ($p < 0.05$) reduction in PGC1α and PGC1β mRNA expression in eWAT and iWAT that was not affected by MnTBAP treatment (Table 1 **and** Supplementary Table 3). Furthermore, HFD significantly ($p < 0.05$) reduced mRNA expression of fatty acid synthase (FAS) and enhanced stearoyl-CoA desaturase 1 (SCD 1) mRNA in eWAT, consistent with an inhibition of de novo lipogenesis and increased mono-unsaturation of saturated fatty acids. Although not significant, there was a small attenuation of these effects with MnTBAP treatment in eWAT (Table 1). The reduction in de novo lipogenesis with HFD was also observed in iWAT but it was insensitive to MnTBAP treatment (Supplementary Table 3). However, HFD-associated SCD1 mRNA expression was unique to eWAT as the expression of this gene was rather reduced with HFD and not affected by MnTBAP treatment in iWAT (Supplementary Table 3), highlighting depot-specific effects of HFD and MnTBAP.

MnTBAP treatment prevented HFD-induced adipocytes apoptosis and inflammation in eWAT

We next examined cell death and inflammation in eWAT and fount that apoptotic and necrotic nuclei were observed only in HF-fed mice treated with saline (Figure 5a, arrows). Thus, the sum of apoptotic and necrotic nuclei/total nuclei was increased by 3 fold in the HF saline group when compared to NC saline group, an effect that was completely prevented by MnTBAP treatment (Figure 5b). As adipocyte death is often associated with inflammation due to the surrounding of dead cells by macrophages, we measured the number crown-like structures as well as TNFα mRNA expression in eWAT. Crown-like structures were more prevalent in eWAT of HF-fed saline-treated mice but rarely seen in HF-fed MnTBAP-treated animals (Figure 5c). Furthermore, TNFα mRNA was enhanced in eWAT of HF-fed animals treated with saline, an effect attenuated with MnTBAP (Figure 5e).

MnTBAP ameliorated the metabolic milieu but failed to prevent HFD-induced systemic insulin resistance and diabetes

Because MnTBAP treatment attenuated diet-induced visceral adiposity, we hypothesized that it would ameliorate the metabolic milieu and the hormonal profile and improve insulin sensitivity. Indeed, MnTBAP significantly ($p < 0.05$) reduced serum levels of free fatty acids (FFAs) and triglycerides (TGs) ($p=0.09$) (Table 2). Consistent with reduced adiposity, leptin

levels, which were increased by 3 fold with HFD, were reduced by 34% ($p<0.05$) with MnTBAP (Table 2). Our short-term HFD did not influence adiponectin levels, but MnTBAP treatment of NC animals caused a slight but significant reduction in adiponectin levels. Despite these improvements in serum FFAs, TGs and leptin levels, MnTBAP treatment failed to reduce fasting glucose and insulin levels (Figure 6a, b). Furthermore, MnTBAP treatment did not prevent glucose intolerance and insulin resistance as evidenced by increased area under the curve for glucose and insulin tolerance tests compared to saline-treated HF-fed group (Supplementary Figure 5a, b).

MnTBAP treatment failed to rescue HFD-induced mitochondrial dysfunction in skeletal muscle

To explore the mechanisms for persistent insulin resistance with MnTBAP, we examined mitochondrial function in skeletal muscle and showed that MnTBAP treatment failed to rescue the reduction in maximal respiration (VADP) caused by HFD (Figure 6c). Furthermore, ATP/O ratios trended lower in the HF-MnTBAP group (Figure 6d) that was associated with enhanced UCP3 protein content (Supplementary Figure 4a, b).

Discussion

The present study was designed to test whether reducing oxidative stress was able to prevent diet-induced adiposity, insulin resistance and diabetes in mice. The major findings of this study are: (**1**) MnTBAP diminished HFD-induced oxidative stress in eWAT; (**2**) attenuated weight gain and adiposity; (**3**) prevented diet-induced adipocyte death and adipose tissue inflammation; (**4**) improved lipid profile and reduced circulating leptin levels; (**5**) but failed to prevent hyperglycemia and hyperinsulinemia.

Mechanisms of attenuated visceral adiposity with MnTBAP treatment

While low levels of ROS are important for cell signaling, their increase is associated with many diseases. Genetic and nutritional obesity are characterized by increased systemic and adipose tissue oxidative stress but a causal role for ROS in the development of this condition has not been established. Furthermore, ROS are involved in many metabolic alterations associated with obesity such as insulin resistance, diabetes, hepatic steatosis and adipose tissue inflammation (16, 17, 18, 19), thus providing a rational for using antioxidant molecules to prevent these conditions. Here we showed that superoxide production increased in eWAT with short-term HF feeding consistent with prior reports (4, 20). The mechanisms for increased adipose superoxide generation is less well understood but could involve mitochondrial dysfunction (21), reduced antioxidant defense or enhanced NADPH oxidase activity (4). While no defect in mRNA expression of NOX4, Sod1 or GPX4 was observed, a post-transcriptional regulation affecting their enzymatic activity is possible. In contrast, we observed a compensatory increase in mRNA level of Sod2 (MnSOD) with HF feeding, suggesting mitochondria as the primary source for superoxide, that could diffuse to the cytosol in the form of hydrogen peroxide. Nonetheless, superoxide generation as well as the induction of Sod2 gene by HFD was prevented by MnTBAP treatment. In addition to reducing oxidative stress, we showed for the first time that MnTBAP reduced body weights and adiposity. Consistent with our results, Laurent et al (22) showed that MnTBAP

treatment of genetically obese *ob/ob* mice resulted in a modest but significant decrease in weight gain but the underlying mechanisms were not investigated. The effect of MnTBAP on body weight and adiposity in our study was confirmed by the decrease in fat mass, brown adipose tissue (BAT) and eWAT weights and circulating leptin levels. MnTBAP specifically targeted BAT and eWAT which could be due their specific response to HFD. Indeed, both BAT and eWAT are known to expand by hypertrophy through increased lipid accumulation, whereas other depots such as perirenal and iWAT increased mainly by hyperplasia after HFD (23, 24, 25). To investigate the mechanisms by which MnTBAP attenuated HFD-induced obesity, several possibilities were examined. First, MnTBAP had no effect on caloric intake, energy expenditure or physical activity. Second, although we did not assess the effect of MnTBAP treatment on fat absorption, both NC and HF-fed animals treated with this compound showed no clinical evidence of malabsorption as would be seen with induced diarrheal disorders. Furthermore NC-fed animals treated with MnTBAP did not lose weight as you would expect with malabsorption. Third, decreased adiposity with MnTBAP could be caused by reduced adipogenesis and/or increased lypolysis. To test that, we measured mRNA expression of key adipogenic and lipolytic enzymes in eWAT and iWAT. In accordance with prior studies (26, 27), we showed that short-term HFD increased transcription of PPARγ, the master regulator of adipogenesis, as well as one of its downstream targets; the aP2 gene. Interestingly, HF-induced adipogenesis in eWAT was prevented by MnTBAP treatment, which could have participated in the reduction of adiposity. Although it did not reach significance, we observed a slight reduction in mRNA levels of PPARγ, CEBPα and aP2 in NC-fed MnTBAP treated animals, which suggest that scavenging physiological levels of ROS could inhibit adipogenesis *in-vivo* as it was previously reported *in-vitro* (28). In addition to reducing the adipogenic program, MnTBAP diminished HF-induced adipocyte hypertrophy as evidenced by smaller adipocyte diameter. This could be due to increased lipolysis, reduced fat intake or enhanced fat oxidation. Basal lipolysis was unaffected by MnTBAP treatment, as evidenced by normal mRNA level of HSLs and reduced rather than increased circulating FFAs. However, assessing mRNA levels is not sufficient to draw a definite conclusion on lypolisis, thus further studies are needed to address whether catecholamine-stimulated lipolysis is different between saline-treated and MnTBAP-treated mice fed HFD. In contrast to lipolysis, mRNA levels of fatty acid translocase CD36 was enhanced in saline-treated but not in MnTBAP-treated mice fed HFD, suggesting that CD36-facilitated fatty acid (FA) uptake, known to increase with HF feeding (29), was reduced with MnTBAP treatment leading to smaller adipocytes. Despite less FA uptake with MnTAP, we did not observe an increase in circulating levels of FFAs and TGs, if anything they were reduced with the treatment raising the possibility for higher FA utilization. Finally, genes involved in fatty acid oxidation and mitochondrial function were similarly altered by HFD in saline and MnTBAP-treated animals respectively whereas genes involved in de novo lipogenesis decreased only in HF-fed saline treated animals.

Mechanisms of prevented adipocyte death and inflammation in eWAT

Adipose tissue inflammation is often associated with oxidative stress, adipocyte death and the scavenging of dead adipocytes by pro-inflammatory macrophages (19). We tested the hypothesis that MnTBAP treatment protects against adipocyte death and inflammation. Indeed, we detected more adipocyte death, more crown-like structures and higher TNFα

mRNA expression in eWAT of HF-fed saline-treated mice but not in HF-fed MnTBAP-treated animals. This is to our knowledge the first report to show that the use of a SOD mimetic is capable of alleviating inflammation and reducing cell death in white adipose tissue. The mechanism by which MnTBAP reduced cell death and adipose tissue inflammation could be related to reduce adipocytes hypertrophy. Indeed, adipocytes hypertrophy creates areas of local adipose tissue hypoxia which in turn could trigger the expression of genes involve in inflammation and matrix remodeling (30). Although we did not detect any difference in HIF1α mRNA (data not shown) the stabilization of this protein was not investigated. Furthermore, HF-induced PAI-1 mRNA expression in eWAT was completely prevented by MnTBAP treatment (data not shown), supporting that MnTBAP reduced adipose tissue remodeling.

Short-term treatment with MnTAP did not prevent HFD-induced systemic insulin resistance and diabetes

Prior studies have associated oxidative stress to the development of insulin resistance. Indeed, it was proposed that ROS are causal in the development of insulin resistance in 3T3-L1 preadipocytes exposed to TNFα or dexamethasone (31) and in L6 myotubes rendered insulin resistant by exposure to palmitate (32). Furthermore, reducing hydrogen peroxide emission through the use of mitochondria-targeted small peptide antioxidant (SS31) attenuated HFD-induced insulin resistance *in-vivo* (33). In addition, chronic treatment of genetically obese and insulin resistant *ob/ob* mice with MnTBAP improved insulin sensitivity and glucose tolerance without affecting body weights (31) and animals with enhanced antioxidant capacity such as mice over-expressing mitochondria-targeted catalase, MnSOD, or mice with MnSOD gene delivery in skeletal muscle were either completely or partially protected against aging or HFD-induced glucose intolerance and insulin resistance (32, 34, 35). In contrast to these studies, other investigations were unable to confirm a causal role for oxidative stress in the etiology of insulin resistance specifically under conditions of higher caloric intake. For example, Paglialunga et al (36) showed that the use of mitochondria-targeted antioxidant SKQ failed to improve HFD-induced insulin resistance despite reduced oxidative stress in skeletal muscle. Furthermore, mice lacking glutathione peroxidase 1 (GPX1) and exhibiting higher hydrogen peroxide levels are protected against HFD-induced insulin resistance (37). In the present study, we extended our previously published studies showing that protection against oxidative stress in FVB mice reduced weight gain but did not prevent insulin resistance after HFD (10) by demonstrating that scavenging ROS by the use of a SOD mimetic attenuated adiposity and weight gain but was not able to prevent insulin resistance and diabetes. Thus, animals treated with MnTBAP and fed HFD still exhibit fasting hyperglycemia, hyperinsulinemia and increased area under the curve of glucose and insulin tolerance tests, raising the question whether ROS are causal for development of insulin resistance and diabetes. Taken together, these results suggest that while reducing ROS levels could reduce weight gain, adiposity and adipose tissue remodeling other mechanisms might be involved in the development of glucose intolerance and insulin resistance in response to short-term HF feeding. Some of these mechanisms may include impaired skeletal muscle glucose uptake, irreversible mitochondrial dysfunction, reduced mitochondrial content, altered mitochondrial dynamics or that the treatment was not long enough to reverse glucose intolerance and insulin sensitivity. Although, we did not

investigate muscle glucose uptake in the present study, we examined mitochondrial function in saponin-permeabilized soleus fibers and observed a reduction in ADP-stimulated respiration in HF-fed saline-treated group, that was not recovered by MnTBAP treatment, thus the ATP/O ratios trended lower in HF-fed MnTBAP-treated samples, suggesting a slight uncoupling of the electron transport chain that could limit ATP availability for muscle glucose uptake (38). In conclusion, this study highlights a role for ROS in the development of diet-induced visceral adiposity but not insulin resistance and diabetes.

In summary, these results highlight the role of oxidative stress in the etiology of weight gain caused by HF feeding but not in the development of the associated insulin resistance. Furthermore, these studies reveal novel redox-sensitive pathways involved in visceral adipose tissue expansion and hepatic steatosis caused by dietary obesity and that could be targeted by antioxidant treatment.

Study limitation

We acknowledge that there are limitations in these studies such as the type and the duration of the diet used. Indeed, the NC and the HFD used in these studies are not isocaloric as the amount of calories obtained some components of the diet (carbohydrates) is not similar and the composition of these components is also different.

Supplementary Material

Refer to Web version on PubMed Central for supplementary material.

Acknowledgments

References

1. Cynthia L. Ogden MDC BKKaKMF. Prevalence of Obesity in the Unites States, 2009-2010. NCHS Data Brief. 2012; 82:1–8. [PubMed: 22617494]

2. Despres JP, Lemieux I. Abdominal obesity and metabolic syndrome. Nature. 2006; 444:881–887. [PubMed: 17167477]

3. Keaney JF Jr, Larson MG, Vasan RS, Wilson PW, Lipinska I, Corey D, et al. Obesity and systemic oxidative stress: clinical correlates of oxidative stress in the Framingham Study. Arterioscler Thromb Vasc Biol. 2003; 23:434–439. [PubMed: 12615693]

4. Furukawa S, Fujita T, Shimabukuro M, Iwaki M, Yamada Y, Nakajima Y, et al. Increased oxidative stress in obesity and its impact on metabolic syndrome. J Clin Invest. 2004; 114:1752–1761. [PubMed: 15599400]

5. Lee YS, Kim AY, Choi JW, Kim M, Yasue S, Son HJ, et al. Dysregulation of adipose glutathione peroxidase 3 in obesity contributes to local and systemic oxidative stress. Mol Endocrinol. 2008; 22:2176–2189. [PubMed: 18562625]

6. Pasternack RF, Banth A, Pasternack JM, Johnson CS. Catalysis of the disproportionation of superoxide by metalloporphyrins. III. J Inorg Biochem. 1981; 15:261–267. [PubMed: 6273505]

7. Faulkner KM, Liochev SI, Fridovich SI. Stable Mn(III) porphyrins mimic superoxide dismutase in vitro and substitute for it in vivo. J Biol Chem. 1994; 269:23471–23476. [PubMed: 8089112]

8. Day BJ, Shawen S, Liochev SI, Crapo JD. A metalloporphyrin superoxide dismutase mimetic protects against paraquat-induced endothelial cell injury, in vitro. J Pharmacol Exp Ther. 1995; 275:1227–1232. [PubMed: 8531085]

9. Day BJ, Crapo JD. A metalloporphyrin superoxide dismutase mimetic protects against paraquatinduced lung injury in vivo. Toxicol Appl Pharmacol. 1996; 140:94–100. [PubMed: 8806874]

10. Boudina S, Sena S, Sloan C, Tebbi A, Han YH, O'Neill BT, et al. Early mitochondrial adaptations in skeletal muscle to diet-induced obesity are strain dependent and determine oxidative stress and energy expenditure but not insulin sensitivity. Endocrinology. 2012; 153:2677–2688. [PubMed: 22510273]

11. Tabbi-Anneni I, Cooksey R, Gunda V, Liu S, Mueller A, Song G, et al. Overexpression of nuclear receptor SHP in adipose tissues affects diet-induced obesity and adaptive thermogenesis. Am J Physiol Endocrinol Metab. 2010; 298:E961–970. [PubMed: 20124506]

12. Nishimura S, Manabe I, Nagasaki M, Hosoya Y, Yamashita H, Fujita H, et al. Adipogenesis in obesity requires close interplay between differentiating adipocytes, stromal cells, and blood vessels. Diabetes. 2007; 56:1517–1526. [PubMed: 17389330]

13. Boudina S, Sena S, O'Neill BT, Tathireddy P, Young ME, Abel ED. Reduced mitochondrial oxidative capacity and increased mitochondrial uncoupling impair myocardial energetics in obesity. Circulation. 2005; 112:2686–2695. [PubMed: 16246967]

14. Perez-Echarri N, Noel-Suberville C, Redonnet A, Higueret P, Martinez JA, Moreno-Aliaga MJ. Role of adipogenic and thermogenic genes in susceptibility or resistance to develop diet-induced obesity in rats. J Physiol Biochem. 2007; 63:317–327. [PubMed: 18457007]

15. Ho JN, Son ME, Lim WC, Lim ST, Cho HY. Anti-obesity effects of germinated brown rice extract through down-regulation of lipogenic genes in high fat diet-induced obese mice. Biosci Biotechnol Biochem. 2012; 76:1068–1074. [PubMed: 22790925]

16. Lu SC. Antioxidants in the treatment of chronic liver diseases: why is the efficacy evidence so weak in humans? Hepatology. 2008; 48:1359–1361. [PubMed: 18697215]

17. Giacco F, Brownlee M. Oxidative stress and diabetic complications. Circ Res. 2010; 107:1058–1070. [PubMed: 21030723]

18. Fridlyand LE, Philipson LH. Reactive species and early manifestation of insulin resistance in type 2 diabetes. Diabetes Obes Metab. 2006; 8:136–145. [PubMed: 16448517]

19. Sun K, Kusminski CM, Scherer PE. Adipose tissue remodeling and obesity. J Clin Invest. 2011; 121:2094–2101. [PubMed: 21633177]

20. Jobgen W, Fu WJ, Gao H, Li P, Meininger CJ, Smith SB, et al. High fat feeding and dietary Larginine supplementation differentially regulate gene expression in rat white adipose tissue. Amino Acids. 2009; 37:187–198. [PubMed: 19212806]

21. Wilson-Fritch L, Nicoloro S, Chouinard M, Lazar MA, Chui PC, Leszyk J, et al. Mitochondrial remodeling in adipose tissue associated with obesity and treatment with rosiglitazone. J Clin Invest. 2004; 114:1281–1289. [PubMed: 15520860]

22. Laurent A, Nicco C, Tran Van Nhieu J, Borderie D, Chereau C, Conti F, et al. Pivotal role of superoxide anion and beneficial effect of antioxidant molecules in murine steatohepatitis. Hepatology. 2004; 39:1277–1285. [PubMed: 15122756]

23. Lemonnier D. Effect of age, sex, and sites on the cellularity of the adipose tissue in mice and rats rendered obese by a high-fat diet. J Clin Invest. 1972; 51:2907–2915. [PubMed: 5080416]

24. Joe AW, Yi L, Even Y, Vogl AW, Rossi FM. Depot-specific differences in adipogenic progenitor abundance and proliferative response to high-fat diet. Stem Cells. 2009; 27:2563–2570. [PubMed: 19658193]

25. Levin BE, Finnegan MB, Marquet E, Triscari J, Comai K, Sullivan AC. Effects of diet and obesity on brown adipose metabolism. Am J Physiol. 1984; 246:E418–425. [PubMed: 6326610]

26. Kim S, Jin Y, Choi Y, Park T. Resveratrol exerts anti-obesity effects via mechanisms involving down-regulation of adipogenic and inflammatory processes in mice. Biochem Pharmacol. 2011; 81:1343–1351. [PubMed: 21439945]

27. Zhou CJ, Huang S, Liu JQ, Qiu SQ, Xie FY, Song HP, et al. Sweet tea leaves extract improves leptin resistance in diet-induced obese rats. J Ethnopharmacol. 2012

28. Tormos KV, Anso E, Hamanaka RB, Eisenbart J, Joseph J, Kalyanaraman B, et al. Mitochondrial complex III ROS regulate adipocyte differentiation. Cell Metab. 2011; 14:537–544. [PubMed: 21982713]

29. Hegarty BD, Cooney GJ, Kraegen EW, Furler SM. Increased efficiency of fatty acid uptake contributes to lipid accumulation in skeletal muscle of high fat-fed insulin-resistant rats. Diabetes. 2002; 51:1477–1484. [PubMed: 11978645]

30. Hosogai N, Fukuhara A, Oshima K, Miyata Y, Tanaka S, Segawa K, et al. Adipose tissue hypoxia in obesity and its impact on adipocytokine dysregulation. Diabetes. 2007; 56:901–911. [PubMed: 17395738]

31. Houstis N, Rosen ED, Lander ES. Reactive oxygen species have a causal role in multiple forms of insulin resistance. Nature. 2006; 440:944–948. [PubMed: 16612386]

32. Hoehn KL, Salmon AB, Hohnen-Behrens C, Turner N, Hoy AJ, Maghzal GJ, et al. Insulin resistance is a cellular antioxidant defense mechanism. Proc Natl Acad Sci U S A. 2009; 106:17787–17792. [PubMed: 19805130]

33. Anderson EJ, Lustig ME, Boyle KE, Woodlief TL, Kane DA, Lin CT, et al. Mitochondrial H2O2 emission and cellular redox state link excess fat intake to insulin resistance in both rodents and humans. J Clin Invest. 2009; 119:573–581. [PubMed: 19188683]

34. Lee HY, Choi CS, Birkenfeld AL, Alves TC, Jornayvaz FR, Jurczak MJ, et al. Targeted expression of catalase to mitochondria prevents age-associated reductions in mitochondrial function and insulin resistance. Cell Metab. 2010; 12:668–674. [PubMed: 21109199]

35. Boden MJ, Brandon AE, Tid-Ang JD, Preston E, Wilks D, Stuart E, et al. Overexpression of manganese superoxide dismutase ameliorates high-fat diet-induced insulin resistance in rat skeletal muscle. Am J Physiol Endocrinol Metab. 2012; 303:E798–805. [PubMed: 22829583]

36. Paglialunga S, van Bree B, Bosma M, Valdecantos MP, Amengual-Cladera E, Jorgensen JA, et al. Targeting of mitochondrial reactive oxygen species production does not avert lipid-induced insulin resistance in muscle tissue from mice. Diabetologia. 2012; 55:2759–2768. [PubMed: 22782287]

37. Loh K, Deng H, Fukushima A, Cai X, Boivin B, Galic S, et al. Reactive oxygen species enhance insulin sensitivity. Cell Metab. 2009; 10:260–272. [PubMed: 19808019]

38. Jheng HF, Tsai PJ, Guo SM, Kuo LH, Chang CS, Su IJ, et al. Mitochondrial fission contributes to mitochondrial dysfunction and insulin resistance in skeletal muscle. Mol Cell Biol. 2012; 32:309–319. [PubMed: 22083962]

What is known about this subject

Systemic and adipose tissue oxidative stress is enhanced in obese humans and animals

Antioxidants have been used to reduce insulin resistance and the metabolic syndrome

Some antioxidants have been shown to reduce weight gain in animals

What does this study add

This study is the first to report that reduced oxidative stress through the use of a superoxide dismutase mimetic (MnTBAP) attenuates high fat diet-induced adiposity

It provides mechanisms by which MnTBAP attenuates visceral adiposity, which was previously unknown

It dissociates the beneficial effect of MnTBAP on adiposity and adipose tissue inflammation from the development of diet-induced insulin resistance and diabetes
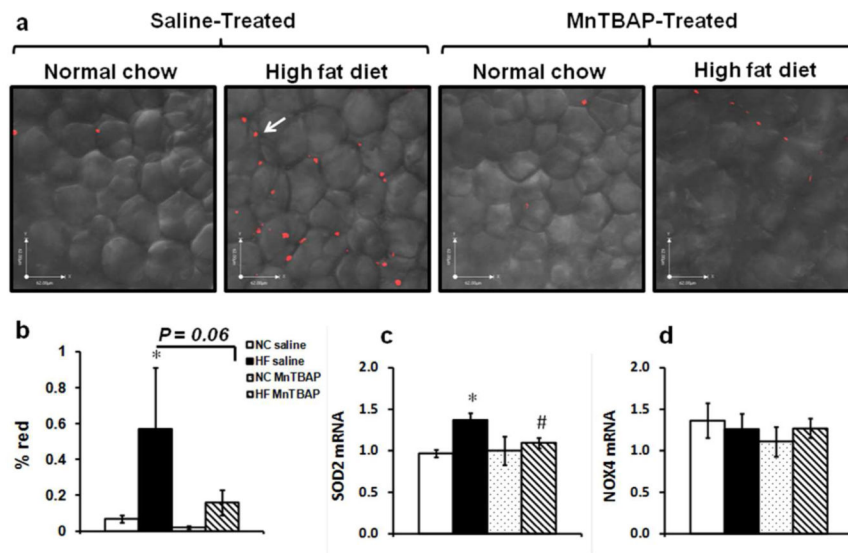
Figure 1.
MnTBAP treatment effectively reduced HFD-induced oxidative stress in epididymal white adipose tissue (eWAT). (**a**) Freshly isolated eWAT sections stained with the superoxide detector MitoSOX red and (**b**) the % red fluorescence (arrows) was quantified in three low-power field images from five animals in each group. NC: normal chow; HF: high fat. (**c**) and (**d**) mRNA expression of Sod2 (MnSOD) and NADPAH oxidase 4 (NOX 4) respectively in eWAT. Data are mean ± SEM; n=5 mice per group for MitoSOX and n= 5-8 mice per group for mRNA. * $P < 0.05$ vs NC of the same treatment, # $P < 0.05$ vs saline under the same feeding condition.
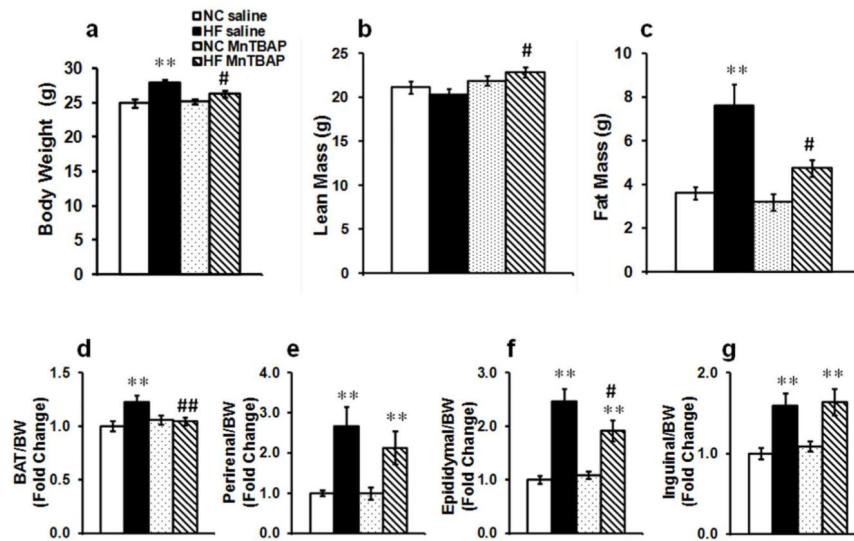
Figure 2.
MnTBAP prevented HFD-induced weight gain and visceral adiposity. (**a**) Body weights, (**b**) lean mass, (**c**) fat mass, (**d**) brown adipose tissue (BAT) weight/body weight (BW), (**e**) perirenal weight/BW, (**f**) epididymal weight/BW and (**g**) inguinal weight/BW. Data are mean ± SEM; *n*=15-18 mice per group for (**a**), (**b**), (**c**), (**d**), (**f**) and (**g**), *n*= 8 mice per group for (**e**). * *P < 0.05*; ** *P < 0.005* vs NC of the same treatment, # *P < 0.05*; ## *P < 0.005* vs saline under the same feeding condition.
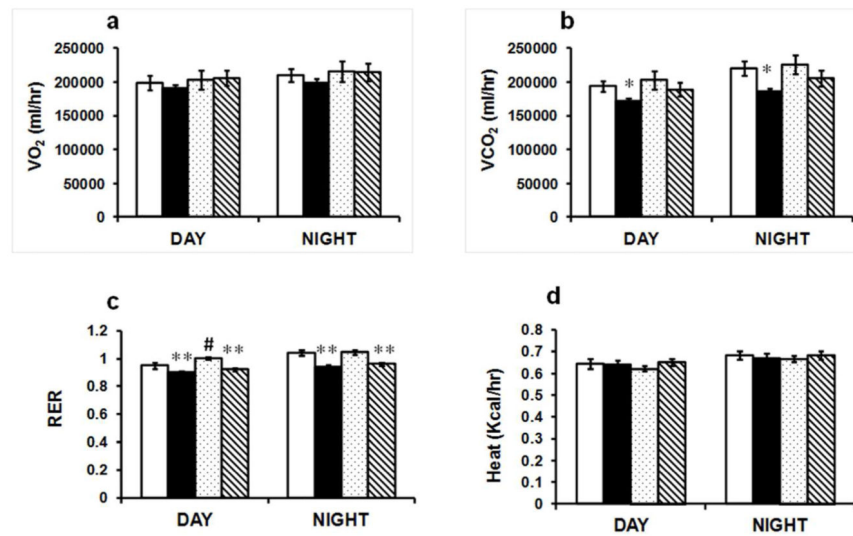
Figure 3.
The effect of MnTBAP on whole body energy homeostasis. (**a**) Oxygen consumption (VO_2).
(**b**) Carbon dioxide release (VCO_2). (**c**) Respiratory exchange ratio (RER). (**d**) Heat
production. Values represent averages of three consecutive days and nights. Data are mean ±
SEM; *n*=6 mice per group. * *P < 0.05*; ** *P < 0.005* vs NC of the same treatment, # *P < 0.05*
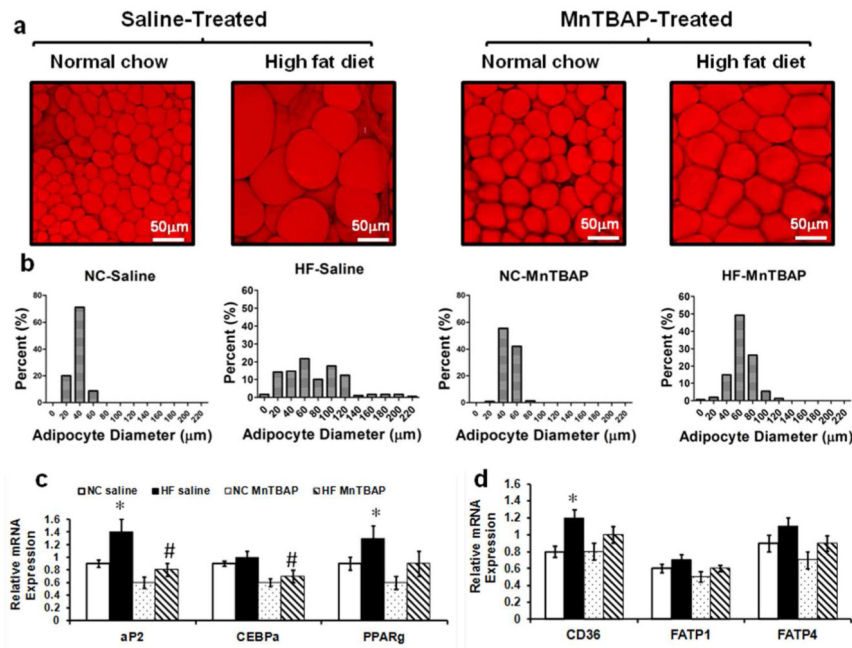vs saline under the same feeding condition.

Figure 4.
MnTBAP treatment reduced HFD-induced adipocyte hypertrophy and expression of genes that regulates adipogenesis and fatty acid uptake. (**a**) Representative images of eWAT stained with the lipid stain BODIPY. (**b**) Adipocyte diameter distribution assessed on at least ten low-power field images that were acquired at regular intervals form five animals in each group. (**c**) eWAT mRNA expression of genes encoding key proteins and transcription factors involved in adipogenesis (such as aP2, CEBPα and PPARγ). (**d**) eWAT mRNA expression of genes encoding proteins involved in fatty acid transport (such as CD36, FATP1 and FATP4). Data are mean ± SEM; n=5 mice per group for (**a**) and (**b**) and n=6-8 mice per group for (**c**) and (**d**). * $P < 0.05$ vs NC of the same treatment, # $P < 0.05$ vs saline under the same feeding condition.
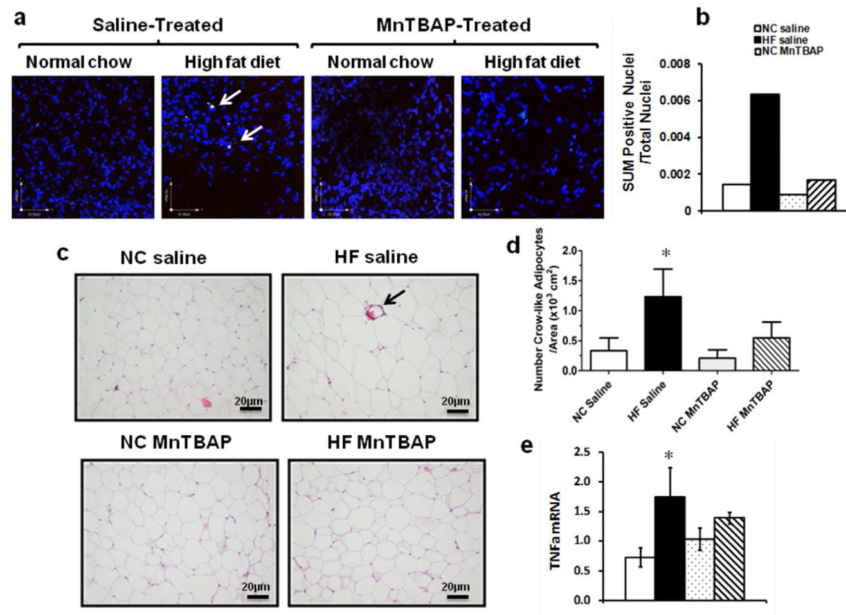
Figure 5.
MnTBAP treatment attenuated adipocyte death and reduced inflammation in eWAT. (**a**) Representative images of eWAT sections stained with apoptotic nuclei stain YO-PRO-1 (green) and the cell death stain propidium iodide (PI) (red). The overlap between green and red is represented (arrows). (**b**) The sum of dead nuclei positive for both YO-PRO-1 and PI over total nuclei. At least 1000 nuclei were counted per animal for three animals per group at randomly chosen sections. (**c**) Representative eWAT sections stained with Hematoxylin and Eosin and showing crown-like structures (arrow). (**d**) Crown-like structures quantification per area on at least 5 images per mouse. (**d**) TNFα mRNA expression in eWAT. Data are mean ± SEM; n=3-4 mice per group for (**a**), (**b**), (**c**) and (**d**), n=5-7 mice per group for (**d**). * $P < 0.05$ vs NC of the same treatment.
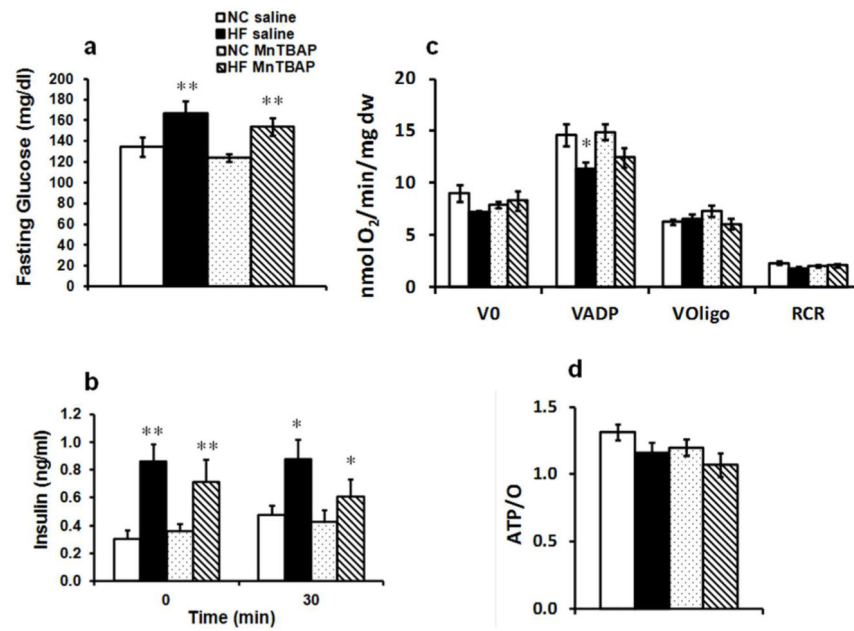
Figure 6.
MnTBAP treatment failed to improve insulin resistance caused by HF feeding. (**a**) Fasting glucose and (**b**) fasting insulin levels measured at baseline and after glucose challenge during glucose tolerance tests. (**c**) Oxygen consumption of saponin-permeabilized soleus muscle fibers in the presence of succinate (5 mmol/L) and rotenone (10 µmol/L) (V0), after addition of 1 mmol/L ADP (VADP) and after inhibition of ATP synthase with 1µg/L oligomycin (Voligo). RCR is the respiratory control ratio of VADP/Voligo. (**d**) ATP/O ratios obtained by dividing ATP synthesis rates over VADP. Data are mean ± SEM; n=14-17 mice per group for (**a**) and n=7-17 mice per group for (**b**); n=5-8 mice per group for (**c**) and (**d**). * $P < 0.05$; ** $P < 0.005$ vs NC of the same treatment.

Table 1

Expression of fatty acid oxidation, fatty acid synthesis, de novo lipogenesis and lypolysis genes in epididymal white adipose tissue

	NC saline	HF saline	NC MnTBAP	HF MnTBAP
Fatty acid oxidation and mitochondrial function				
PGC1α	2.1 ± 0.1	1.5 ± 0.2[*]	1.8 ± 0.2	1.5 ± 0.2
PGC1β	1.6 ± 0.2	1.3 ± 0.1[*]	2 ± 0.2	1.5 ± 0.1[*]
CPT2	1.4 ± 0.1	1.5 ± 0.2	1.5 ± 0.2	1.5 ± 0.1
ACSL1	1.3 ± 0.1	1.2 ± 0.2	1.3 ± 0.2	1 ± 0.04
ACSL5	1.1 ± 0.1	1.3 ± 0.2	1.5 ± 0.2	1.2 ± 0.1
Fatty acid synthesis and de novo lipogenesis				
FAS	1.4 ± 0.1	0.8 ± 0.1[*]	1.2 ± 0.2	1.1 ± 0.2
ACC2	1.4 ± 0.1	1 ± 0.1	1.1 ± 0.2	1 ± 0.1
SCD1	1.3 ± 0.1	1.8 ± 0.4[*]	1± 0.3	1.5 ± 0.1
Lipolysis				
HSL1/2	0.9 ± 0.06	0.9 ± 0.07	0.9 ± 0.2	0.9 ± 0.04
HSL2	1.3 ± 0.07	1.4 ± 0.1	1.2 ± 0.2	1.3 ± 0.07

mRNA was extracted from epididymal white adipose tissue of mice fed normal chow (NC) or high fat (HF) diet and treated with either saline or MnTBAP for 5 weeks starting at 10 weeks of age. mRNA expression was normalized to 16s ribosomal RNA expression which was not significantly different among the groups. NC: normal chow; HF: high fat. Data are expressed as mean ± SEM; n=7-8 mice per group.

[*] $P < 0.05$ vs NC of the same treatment.

Table 2

Serum metabolites and hormones level

	NC saline	HF saline	NC MnTBAP	HF MnTBAP
Triglycerides (mg/dl)	7.4 ± 1.1	16.7 ± 2.6*	10.8 ± 1.8	12.1 ± 2.2
Free Fatty Acids (mM)	0.4 ± 0.04	0.7 ± 0.1	0.5 ± 0.09	0.5 ± 0.03#
Leptin (ng/ml)	3 ± 0.2	9.9 ± 1.7**	3.9 ± 0.9	6.6 ± 1**#
Adiponectin (µg/ml)	5.4 ± 0.6	5.1 ± 0.6	3.4 ± 0.4#	4.9 ± 0.4

Serum metabolites and hormone levels were measured after a 6-hr fast. All metabolites and hormones were determined on blood samples extracted before glucose injection prior to the glucose tolerance tests. NC: normal chow; HF: high fat. Data are expressed as mean ± SEM; n=4-12 mice per group.

*
P < 0.05;

**
P < 0.05 vs NC of the same treatment,

#
P < 0.05 vs saline under the same feeding condition.